Proceedings of the 21st ICSMGE, Vienna, Austria, 14 – 19 June 2026. Pistrol, Adam & Schweiger (eds.)
Published by: ÖGG, Austrian Society for Geomechanics, Salzburg, Austria, ISBN 978-3-9503898-4-5
https://doi.org/10.53243/ICSMGE2026-496

Discussion on stiffness parameters for Hardening Soil and Hardening Soil-Small strain constitutive models based on results of laboratory tests

Magdalena Kowalska
Department of Geotechnics and Roads, Silesian University of Technology, Poland, magdalena.kowalska@polsl.pl

Matylda Tankiewicz
Department of Civil Engineering, Wrocław University of Environmental and Life Sciences, Poland

ABSTRACT: Hardening Soil (HS) and Hardening Soil-Small strain (HSS) have become the most widely used constitutive models in numerical analysis of advanced geotechnical engineering problems. The long list of physical and mechanical parameters of HSS includes several parameters referring to soil stiffness – among others, these are: an initial shear modulus (G_0) or Young's modulus (E_0), a stiffness modulus at 50% of maximum stress intensity (E_{50}), a stiffness modulus under unloading/reloading conditions (E_{ur}), an oedometric modulus (E_{oed}), and an exponent m describing the relationship between stiffness and applied stress. Assessing the entire data set is not easy, fast, or cheap. Well-qualified personnel is needed to perform high-quality in situ or laboratory tests, and to interpret the data. Especially troublesome, due to ambiguous procedures, is the determination of E_{ur} and m. Therefore, software users tend to use default settings or commonly used assumptions. In this study, triaxial, oedometric, and bender element tests were conducted on two soils that are poorly represented in the literature: a loess-sand mixture and a fluvial sand with fines. The parameters E_0, E_{50}, E_{ur}, E_{oed}, and m were assessed using various methods. The results confirmed that the known relationships: (*a*) $E_0 > E_{ur} > E_{50}$ and (*b*) $E_{ur}/E_{50} \approx$ 3-4 are valid for the soils tested. On the other hand, the assumptions that (*c*) $E_{50} \approx E_{oed}$, and that (*d*) the choice of stiffness modulus has a negligible influence on m, were not fulfilled. It was also proved that E_{ur} is highly dependent on the methodology of its estimation.

KEYWORDS: elastic modulus, Hardening Soil, Hardening Soil-Small, loess, oedometric modulus, sand, stiffness.

1 INTRODUCTION

In practice, Hardening Soil (HS) and Hardening Soil-Small strain (HSS) belong to the advanced constitutive models that are currently most often used to simulate soil behaviour in the pre-failure state of stress. HS is an elasto-plastic model developed by Schanz et al. (1999), incorporating multi-surface yield criterion with plastic shear and volumetric hardening. HSS is an extension of the HS model, introduced by Benz (2007, 2009), with improved definition of stiffness non-linearity at small strains. Both models are implemented in the popular commercial finite element modelling (FEM) codes, such as PLAXIS (PLAXIS, 2024) and ZSoil (Obrzud & Truty, 2020). HSS is believed to well describe soil behaviour under static and cyclic loading conditions, although in the latter case some researchers recommend caution due to significant overestimation of stiffness at small strain reversals (Cudny & Truty, 2020; Obrzud & Truty, 2020).

A proper description of soil stiffness is one of the most complex tasks in advanced numerical modelling and often requires the identification of several different parameters. The long list of physical and mechanical parameters of HS includes five parameters referring to soil stiffness: secant stiffness modulus at 50% of the maximum stress intensity (E_{50}), a secant stiffness modulus and a Poisson's ratio under unloading/reloading conditions (E_{ur} and ν_{ur}), an oedometric modulus (E_{oed}), and an exponent m describing the relationship between stiffness, stress and shear strength. HSS requires two more: an initial (maximum) tangent shear modulus (G_0) or Young's modulus (E_0) and a shear strain at which the secant shear modulus is reduced by 27.8% ($\gamma_{0.7}$). The minimum program to assess all these parameters in laboratory campaign includes:

- three triaxial (TX) tests including isotropic consolidation at different effective minor principal stresses σ'_3 and drained shearing with on-sample measurement of strains and one unloading-reloading (U-R) loop at a reference stress σ'^{ref}_3 – to determine E_{50}, E_{ur}, ν_{ur} and m;
- bender element (BE) or resonant column (RC) tests at σ'^{ref}_3 – to determine $\gamma_{0.7}$ and E_0 based on shear wave (S-wave) velocity V_S, and
- one oedometric (OED) test to identify E_{oed} from the virgin compression curve.

The identification procedures are not always clear and unambiguous; for example, the range of strain or stress in the TX test, at which the U-R loop should be executed, is not clearly defined, leaving room for various interpretations.

To simplify the analysis or decrease its cost, the software users often apply some common assumptions and/or use the default settings available in the software. For example, to avoid expensive BE or RC tests, it might be assumed that E_0 can be determined from the initial part of the U-R loop in TX tests, as presented in several software manuals, but this approach is hardly feasible given the precision of the strain measurement in standard TX tests. If the U-R loop from TX tests is not available, in some studies E_{ur} is estimated based on an U-R loop from the OED test (Rebolledo et al., 2019; Surarak et al., 2012).

A variety of data can be found in the literature on the proportions between the various elastic moduli and recommendations on how to calculate the missing parameters in the case of limited experimental data. In general, it is agreed that at σ'^{ref}_3: $E_0 > E_{ur} > E_{50}$. ZSoil users are encouraged to double-check the following relationships: $E_{ur}/E_{50} > 2$ and $3.6 < E_0/E_{50} < 30$ (Obrzud & Truty, 2020). In the manual, it is suggested to assume: E_{ur}/E_{50} between 2 and 6 (in the absence of experimental data, 3 is recommended for sands and 4 for clays), and $E_{50} \approx E_{oed}$. In PLAXIS (2024), E_{ur}/E_{50} is set by default equal to 3 and E_{50}/E_{oed} equal to 1, regardless of the type of soil. These values sometimes differ much from evidence, e.g., for soft lacustrine soils Kempfert & Gebreselassie (2006) obtained E_{ur}/E_{50} between 5.9 and 12.7 and E_{50}/E_{oed} between 0.77 and 1.43. Vermeer and Meier (1998) reported E_{50} greater than E_{oed} in soft soils and lower than E_{oed} for overconsolidated clays.

In HSS, it is assumed that the relationship between any of the stiffness moduli: E_0, E_{ur} or E_{50} and σ'_3 can be described with the following equation involving the coefficient m, cohesion c' and angle of internal friction φ':

$$E = E^{ref}\left(\frac{\sigma'_3 + c' \cdot ctg\varphi'}{\sigma'^{ref}_3 + c' \cdot ctg\varphi'}\right)^m \quad (1)$$

where E^{ref} is the modulus E (E_0, E_{ur} or E_{50}) at selected $\sigma'_3{}^{ref}$ (usually 100 kPa); a similar principle applies to the oedometric modulus (Schanz et al., 1999):

$$E_{oed} = E^{ref}_{oed}\left(\frac{\sigma'_1 + c' \cdot ctg\varphi'}{\sigma'^{ref}_1 + c' \cdot ctg\varphi'}\right)^m \quad (2)$$

where σ'_1 is an effective vertical stress and $E_{oed}{}^{ref}$ is the oedometric modulus at a selected reference vertical stress $\sigma'_1{}^{ref}$.

Usually, the coefficient m is assumed to be 0.5 in sands and silts and 1.0 in soft clays (Janbu, 1963; Schanz et al., 1999). However, several studies show that m cannot be treated as a constant, depending only on the type and state of the soil – its values strongly depend on the identification procedure adopted. For example, for sands and gravels, the exponent based on G_0 (m_0) is generally between 0.4 and 0.6 (Benz, 2007), while the one based on E_{oed}, m_{oed}, is in the range of 0.4 to 0.7 or, slightly higher, i.e., 0.5 to 0.9, at higher fines content (von Soos, 1991). In drained TX tests on soft lacustrine clays, Kempfert & Gebreselassie (2006) obtained m ranging from 0.3 to 0.9 with the largest, medium, and lowest values based on E_0, E_{50} (m_{50}) and E_{ur} (m_{ur}). In OED tests, the same authors obtained m_{oed} in the range of 0.7 to 0.85 at virgin loading and 0.6 to 1.4 from U-R loops. Slightly higher m_{oed} values were shown by Surarak et al. (2012): 0.5 to 1.0 and 1.0 to 1.5, respectively, with higher values for the soft clays and lower values for stiff clays. Oztoprak & Bolton (2013) showed that m increases with strain – this is consistent with the findings of other researchers, since the coefficient m_0 is obtained at very small strains, while m_{50} and m_{oed} at larger strains.

The above examples prove that a simplified approach, in which one stiffness parameter is calculated based on expected relations with some other characteristics, may be misleading. The problem is enhanced in the case of non-textbook soils, for which the number of published studies presenting a complete set of data, enabling verification of the assumptions, is limited. This paper aims to close one of these knowledge gaps by presenting the values of E_0, E_{50}, E_{ur}, E_{oed}, and m for two soils that are poorly represented in the literature: a loess-sand mixture and a clayey sand, and by verifying the generally accepted relationships and correlations in relation to these materials.

2 MATERIAL AND METHODS

The first material was a mixture of loess and medium quartz sand, further referred to as LSM. The loess was acquired from the Sudety forelands deposit in south-west Poland (Lower Silesia). The mixture contained 20.4/63.4/16.1% of the sand/silt/clay fractions. The plastic and liquid limits (fall cone test) of the mixture were equal to: 19.9 and 25.5%, while its mean particle diameter d_{50}, specific gravity, optimum water content and maximum dry density from the standard Proctor test were: 0.36 mm, 2.66 g/cm^3, 11.1% and 1.91 g/cm^3, respectively. The specimens were prepared by compacting the material with standard Proctor energy at optimum moisture content – the details of the procedure can be found in Tankiewicz et al., 2024. The initial void ratio e_0 at the beginning of the tests varied between 0.43 and 0.46.

The second soil was a fluvial sand from southern Poland, hereinafter denoted as FS, containing 6.3/85.3/3.9/4.5% of gravel/sand/silt/clay fractions. Its mean particle diameter, specific gravity, optimum water content, and maximum dry density from the standard Proctor test were equal to: 0.35 mm, 2.68 g/cm^3, 12.5% and 1.81 g/cm^3. The minimum and maximum void ratios were: 0.374 and 0.671, respectively. The specimens were prepared by moist tamping at water content 5% to reach a relative density of 60% (e_0 = 0.493).

The moduli E_0, E_{50}, E_{ur} and E_{oed}, and the exponent m were determined for both materials in oedometric, triaxial, and bender element tests. In OED tests, specimens 63.5 mm (LSM) or 50.5 mm (FS) in diameter and 20 mm in height were compressed at σ'_1 increasing incrementally up to 2000 kPa. Two specimens of each kind were examined. In the TX tests, the fully saturated specimens, 70 mm in diameter and 140 mm in height, were isotropically consolidated at σ'_3 = 50, 100 or 200 kPa and then axially compressed at constant σ'_3 until an axial strain ε_1 reached 15% or until a shear plane formation was visible. For LSM, an additional specimen was sheared drained at σ'_3 = 350 kPa and two more were loaded following vertical effective stress paths, at the constant mean effective stress p' = 200 kPa and 350 kPa. Vertical deformation of the specimens was measured by means of external transducers and on-sample transducers. All classification, oedometric, and triaxial tests were performed in accordance with the EN 13286-2 and ISO 17892 standards. The S-wave velocity was determined in the time domain using BE tests carried out at various levels of σ'_3 during the consolidation stage of the TX tests. The S-wave travel time was estimated for sinusoidal pulse at the excitation frequency for which the start-to-start and peak-to-peak methods gave the same result, cf. Kowalska & Vrettos (2025).

The tangent confined modulus E_{oed} was determined in OED tests from virgin compression curve using equation:

$$E_{oed} = \frac{\delta\sigma'_1}{\delta\varepsilon_1} \quad (3)$$

in which $\delta\sigma'_1$ and $\delta\varepsilon_1$ are the vertical stress and strain increments, respectively, between the next and previous loading steps in relation to the current σ'_1, c.f. Figure 1.

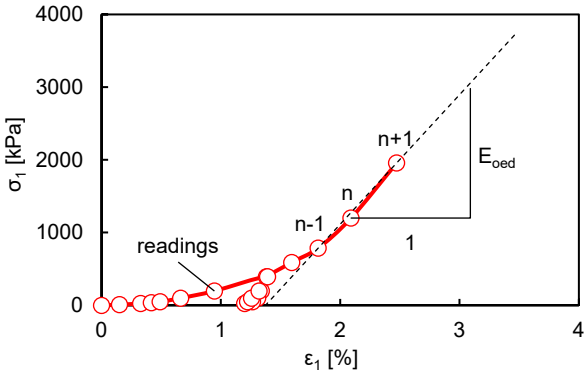

Figure 1. Definition of tangent modulus E_{oed} in OED test: n, n-1, and n+1 are the current, previous, and next loading step.

Additionally, for stresses within the range of normal consolidation, an approximate value of the oedometric modulus, $E_{oed}{}^C$, was estimated based on the compression index C_C from the equation (Obrzud & Truty, 2020):

$$E^C_{oed} = 2.3 \cdot \frac{1 + e_0}{C_C} \cdot \sigma'_1 \quad (4)$$

where e_0 is the initial void ratio of the specimen. The Cc index was calculated as the slope of the best-fit line.

The Young's moduli E in the TX tests were determined using the equation (Lambe & Whitman, 1977):

$$E = \frac{\Delta\sigma'_1 - 2\nu \cdot \Delta\sigma'_3}{\Delta\varepsilon_1} = \frac{\Delta Q}{\Delta\varepsilon_1} \quad (5)$$

where Q is a generalised stress intensity, ν is Poisson's ratio:

$$\Delta Q = \Delta\sigma'_1 - 2\nu \cdot \Delta\sigma'_3 \quad (6)$$

$$\nu = \frac{\Delta\varepsilon_1 \cdot \Delta\sigma'_3 - \Delta\varepsilon_3 \cdot \Delta\sigma'_1}{\Delta\sigma'_3(\Delta\varepsilon_1 - 2\Delta\varepsilon_3) + \Delta\sigma'_1 \cdot \Delta\varepsilon_1} \quad (7)$$

$\Delta\sigma'_1$, $\Delta\sigma'_3$, $\Delta\varepsilon_1$, $\Delta\varepsilon_3$ are the increments of the major and minor principal stresses, and the axial and horizontal strains during the shearing phase, respectively. In the conventional drained TX tests that are carried out under constant effective confining stress, $\Delta\sigma'_3 = 0$ and, hence, $\Delta Q = \Delta\sigma'_1 = \Delta q$.

The modulus E_{50} was calculated in the TX tests as the secant modulus at $\Delta\varepsilon_1$ corresponding to half of the maximum ΔQ (ΔQ_{max}) obtained in the test.

There are no clear instructions on how to execute the U-R loops in TX tests to determine E_{ur}, i.e., at what level of stress or strain the unloading and reloading should start and how to locate the upper point of the loop in case plastic strain occurs at reloading. In this study, a method suggested in the JGS 0542 standard was applied to locate the upper point at the midpoint between points A (start of unloading) and C (return), as presented in Figure 2. The lower point (B) was located at the point of reversal of the stress direction.

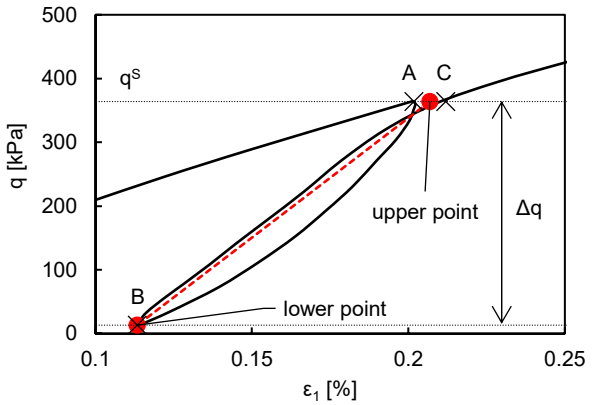

Figure 2. Definition of the parameters of U-R loops in TX tests: upper and lower points, starting stress q^S and stress decrement Δq.

To examine whether the loop parameters have an influence on the measured E_{ur}, loops starting at various levels of q (q^S) and with various decrements of q (Δq), c.f. Figure 2, were applied in selected tests. Some examples are showed in Figure 5 in the results section; for example, at axial compression of the LSM specimen at constant p' = 350 kPa, a series of two loops starting at q^S = 100, 200, 300 and 400 kPa with Δq = 50 kPa and two loops starting at q^S = 200, 300 and 400 kPa with reversals at q = 50 kPa (Δq = 150, 250, 350 kPa) were executed, as presented in Figure 5a (thin purple line).

For comparison, the Young's modulus E_{ur} was also determined from the results of the OED test; hereinafter it is denoted as E_{ur}^{OED}. It was estimated using the concepts of the theory of elasticity and the equation:

$$E_{ur}^{OED} = E_{oed,ur}\frac{(1+\nu_{ur})(1-2\nu_{ur})}{1-\nu_{ur}} \quad (8)$$

where $E_{oed,ur}$ is a modulus obtained from an U-R loop in the OED test and the Poisson's ratio ν_{ur} is assumed constant, equal to 0.2 (a default setting in most FEM codes). Like with E_{ur} in TX tests, there are no unique instructions on how to execute the unloading/reloading phase in OED test and how to determine $E_{oed,ur}$ based on the results. Here, in each test, one U-R loop starting at $\sigma'_1 = \sigma'^S_1$ = 400 kPa was included. The unloading was carried out to 50 kPa and 25 kPa in the tests on LSM and FS, respectively. The $E_{oed,ur}$ at a given stress was determined as the mean value of the tangent moduli at unloading and reloading, determined with the same method as E_{oed} (Figure 1). Like for E_{oed}^C, an approximate value of $E_{oed,ur}$ was also estimated, further denoted as $E_{oed,ur}^C$, based on the swelling index C_S (Obrzud & Truty, 2020):

$$E_{oed,ur}^C = 2.3 \cdot \frac{1+e_0}{C_S} \cdot \sigma'_1 \quad (9)$$

The modulus E_{ur}^{OED} calculated with Equation (8) using $E_{oed,ur}^C$ instead of $E_{oed,ur}$, was denoted as $E_{ur}^{OED,C}$.

To determine the initial Young's modulus E_0 from BE tests, first G_0 was estimated based on V_S and the current bulk density ρ:

$$G_0 = \rho V_S^2 \quad (10)$$

then E_0 was calculated from the equation:

$$E_0 = 2(1+\nu_0) \cdot G_0 \quad (11)$$

where ν_0 is the Poisson's ratio at very small strain. The TX tests were performed on fully saturated specimens; hence, it was impossible to determine ν_0 from the known relationship between shear and compression wave velocities. Therefore, ν_0 was assumed as a constant, equal to 0.2 – such an approach is used in the PLAXIS and ZSoil programs as well.

Based on Equation (1) and Equation (2), the exponents m_0, m_{50}, m_{ur}, m_{oed} were calculated as the slopes of the trendline y = mx + b, where y is the natural logarithm of E_0, E_{50}, E_{ur} or E_{oed}, respectively, and x is the natural logarithm of the ratio (σ' + c'·cotφ')/(σ'^{ref} + c'·cotφ'), where $\sigma' = \sigma'_3$ for m_0, m_{50} and m_{ur}, and $\sigma' = \sigma'_1$ for m_{oed}.

3 RESULTS AND DISCUSSION

The relationships between the void ratio and vertical stress for LSM and FS in the OED tests are presented in Figure 3 and the values of all oedometric moduli at selected σ'^{ref}_1 are shown in Table 1 and Table 2. The C_C and C_S indexes were equal to 0.0588 and 0.0061 in LSM, and 0.0236 and 0.0023 in FS, respectively. Based on Figure 3, the preconsolidation pressure σ'_p in the LSM and FS specimens was estimated at approximately 70 kPa and 200 kPa, respectively, therefore, the E_{oed}^C moduli are valid only at $\sigma'_1 \geq \sigma'_p$.

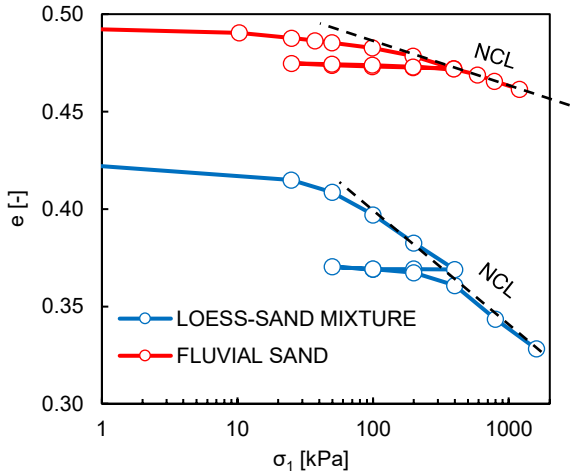

Figure 3. Relationship between void ratio e and vertical stress σ_1 in the OED tests; NCL is the normal consolidation line.

Table 1. Stiffness moduli and their relations from OED tests in LSM.

Moduli	Unit	$\sigma'_1{}^{ref}$ [kPa]				
		50	100	200	400	800
E_{oed}	MN/m^2	6.0*	8.2	15.3	21.9	42.0
$E_{oed,ur}$	MN/m^2	-	132	1225	-	-
$E_{oed}{}^C$	MN/m^2	2.8	5.6	11.2	22.3	44.7
$E_{oed,ur}{}^C$	MN/m^2	26.9	53.8	108	215	431
$E_{oed}/E_{oed}{}^C$	-	-	1.5	1.4	1.0	0.9
$E_{oed,ur}/E_{oed}$	-	-	16	80	-	-

* below preconsolidation pressure

Table 2. Stiffness moduli and their relations from OED tests in FS.

Moduli	Unit	$\sigma'_1{}^{ref}$ [kPa]				
		50	100	200	400	800
E_{oed}	MN/m^2	25.1*	32.4*	41.0	60.6	123
$E_{oed,ur}$	MN/m^2	98.2	175	313	-	-
$E_{oed}{}^C$	MN/m^2	7.3	14.5	29.1	58.2	116
$E_{oed,ur}{}^C$	MN/m^2	74.6	149	299	597	1194
$E_{oed}/E_{oed}{}^C$	-	-	-	1.4	1.0	1.1
$E_{oed,ur}/E_{oed}$	-	3.9	5.4	7.6	-	-

* below preconsolidation pressure

It is clear that the stiffness of FS is significantly larger than that of LSM, which was expected given the much smaller content of fines in FS. As can be seen in Table 1 and Table 2, the approximated moduli $E_{oed}{}^C$ are up to 50% lower than E_{oed}, but the difference becomes negligible when the vertical stress increases. In FS, the stiffness modulus at unloading/reloading is 4 to 8 times higher than at primary loading. In LSM, the $E_{oed,ur}/E_{oed}$ ratio is even higher. This results from a very weak regain of height at unloading, which needs further investigation. When only reloading is considered at $\sigma'_1{}^{ref} = 100$ and 200 kPa, the oedometric modulus is only 3.3 and 8.6 times higher than E_{oed}, respectively, giving a ratio very similar to that in FS. According to Kempfert & Gebreselassie (2006), $E_{oed,ur}$ values depend on the stress at which unloading starts. In this study only one U-R loop was executed; therefore, it was not possible to verify this statement for the soils studied. It should be noted that the Equation (9) enables the calculation of $E_{oed,ur}{}^C$ at all reference stresses and the ratio $E_{oed,ur}{}^C/E_{oed}{}^C$ equals $C_S/C_C \approx 10$.

The stress-strain relationships for LSM and FS in TX tests are presented in Figure 4, while selected U-R loops are shown in Figure 5. Both materials show strong dilatant behaviour. The peak shear strength parameters of LSM are: $c' = 10$ kPa, $\varphi' = 36.1°$, with internal angle of friction at critical state $\varphi'_{cr} = 33.9°$; while in FS they are following: $c' = 7.2$ kPa, $\varphi' = 41.6°$, $\varphi'_{cr} = 33.2°$. The E_{50} values, obtained using the presented plots, are listed in Table 3 and Table 4.

The E_{ur} values calculated for the complete U-R loops (ABC) executed in the TX tests on the LSM specimens showed a very large scatter – see all the grey markers in Figure 6. To examine the influence of the loop's 'relative length', the data were sorted according to the ratio of the stress decrement ΔQ to the stress at which the loop started Q^S. They are showed in Figure 6 using different grey markers: circles, triangles, and squares indicate $\Delta Q/Q^S$ smaller than 0.33, within the range of 0.33 and 0.67, and larger than 0.67, respectively. It can be noticed that the shorter the loop, i.e., the smaller the $\Delta Q/Q^S$ ratio, the greater the stiffness obtained, which is due to the smaller axial strain and the non-linear, hysteretic, behaviour of the soil. Therefore, to unify the approach, it was decided to

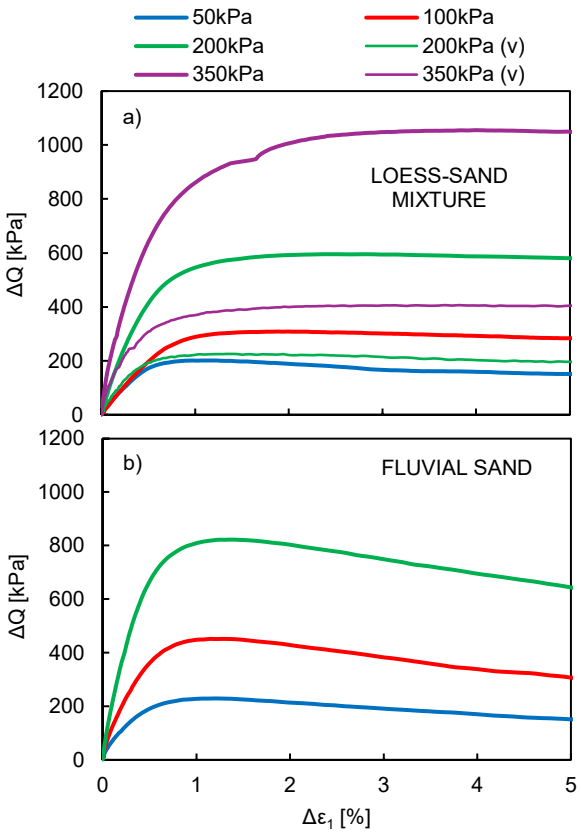

Figure 4. Relationship between increments of vertical strain $\Delta\varepsilon_1$ and generalised stress intensity ΔQ in TX tests on LSM (a) and FS (b); (v) denotes the tests with vertical stress paths; only monotonic loading.

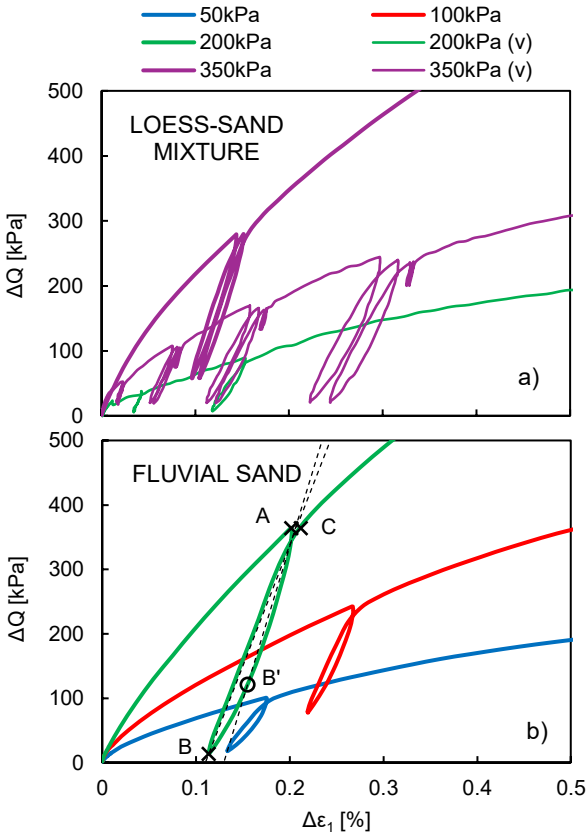

Figure 5. Selected U-R loops in TX tests on LSM (a) and FS (b); (v) denotes the tests with vertical stress paths; points A, B, B' and C are explained in the text; inclination of the black dashed lines refers to E_{ur}.

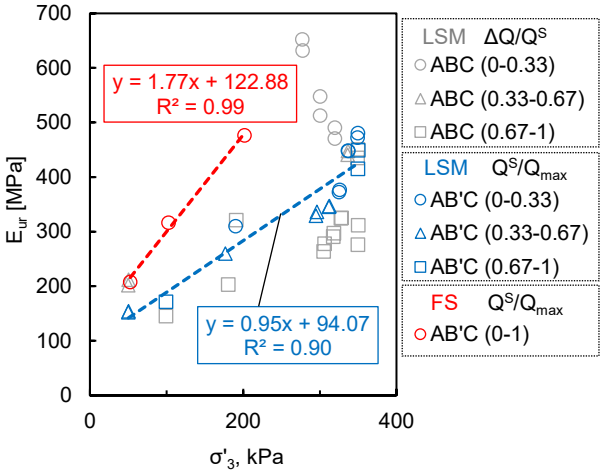

Figure 6. Relationship between E_{ur} and σ'_3 for various types of U-R loops in TX tests on LSM and FS; ABC – original loops, AB'C – corrected loops with $\Delta Q/Q^S$ = 0.33; the meaning of the markers is explained in the text.

ignore the loops in which $\Delta Q/Q^S$ was less than 0.33 and in the others – to take point B', located at 1/3 of Q^S, as the lower point of the loop for the E_{ur} calculation, instead of the original point of reversal (B) – see Figure 5b, i.e. to keep $\Delta Q/Q^S$ = 0.33. The corrected E_{ur} values are presented in Figure 6 with blue markers. These results show a much smaller scatter (R^2 = 0.9 for a linear approximation) and, as expected, clearly increase with σ'_3. To observe whether the level at which the loop is started has an influence on the results, the data were further sorted with regard to the ratio Q^S/Q_{max} – see the blue markers showing results grouped for Q^S/Q_{max} smaller than 0.33 (circles), between 0.33 and 0.67 (triangles) and larger than 0.67 (squares). As can be seen in Figure 6, there is no clear dependency between Q^S/Q_{max} and E_{ur} – this latter observation is consistent with the results presented by Kempfert & Gebreselassie (2006) for soft clays. A similar approach was also applied to the FS results – the E_{ur} moduli obtained are presented in Figure 6 with red markers (without differentiating with respect to Q^S/Q_{max}). The E_{ur} values at four different σ'^{ref}_3 are showed in Table 3 (approximated using the equation showed in Figure 6) and Table 4.

Typical output signals from BE tests in FS and LSM specimens at σ'_3 = 100 kPa are presented in Figure 7. The FS specimens exhibited larger signal disturbance with greater attenuation causing the first wave to have much smaller amplitude than the following waves, which is typical for stiff soils, cf. Gao et al (2022) or Kowalska & Vrettos (2025). The relationship between the G_0 values obtained and the mean effective stress can be described with a simple power law:

$$G_0 = G_{0,100} \cdot \left(\frac{\sigma'_3}{p_a}\right)^{\beta} \qquad (12)$$

where p_a is the atmospheric pressure (100 kPa), $G_{0,100}$ is the initial shear modulus at σ'_3 = 100 kPa, and β is a curve fitting parameter. The values obtained for $G_{0,100}$ and β are equal to: 163.17 MPa and 0.58 for FS, and 120.78 MPa and 0.61 for LSM. The respective coefficients of determination R^2 are 0.996 and 0.987, confirming the suitability of the power law. The E_0 values calculated at selected reference stresses are listed in Table 3 and Table 4.

The relations between various stiffness moduli E_{ur}/E_{50}, E_0/E_{50}, E_0/E_{ur}, E_{50}/E_{oed}, $E_{50}/E_{oed}{}^C$ and $E_{ur}/E_{ur}{}^{OED,C}$ are presented in Table 3 and Table 4. The oedometric moduli E_{oed}, $E_{oed}{}^C$ and $E_{ur}{}^{OED,C}$ were originally determined at selected σ'^{ref}_1 (Table 1

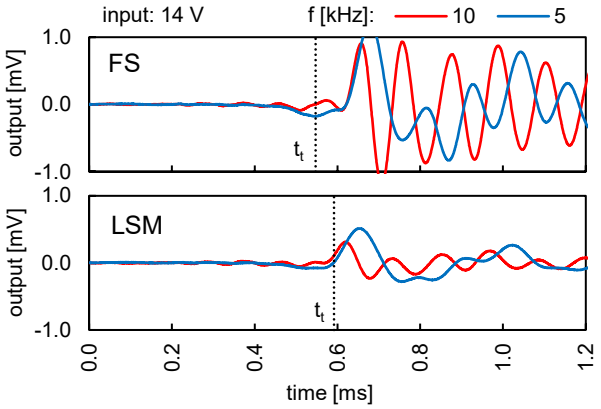

Figure 7. Typical output signal in BE tests; t_t is S-wave travel time.

Table 3. Stiffness moduli E_0, E_{50}, E_{ur}, E_{oed}, $E_{oed}{}^C$, and $E_{ur}{}^{OED,C}$ and their relations in LSM specimens at selected σ'^{ref}_3.

Parameter	Unit	σ'^{ref}_3 [kPa]			
		50	100	200	350
E_0	MN/m²	189.9	289.9	442.5	622.7
E_{ur}	MN/m²	141.4	188.7	283.4	425.4
E_{50}	MN/m²	33.2	53.6	86.6	127.5
E_{oed}	MN/m²	9.8	15.5	27.0	44.3
$E_{oed}{}^C$	MN/m²	6.8	13.6	27.2	47.6
$E_{ur}{}^{OED,C}$	MN/m²	58.9	117.9	235.8	412.6
E_{ur}/E_{50}	-	4.3	3.5	3.3	3.3
E_0/E_{50}	-	5.7	5.4	5.1	4.9
E_0/E_{ur}	-	1.3	1.5	1.6	1.5
E_{50}/E_{oed}	-	3.4	3.5	3.2	2.9
$E_{50}/E_{oed}{}^C$	-	4.9	3.9	3.2	2.7
$E_{ur}/E_{ur}{}^{OED,C}$	-	2.4	1.6	1.2	1.0

Table 4. Stiffness moduli E_0, E_{50}, E_{ur}, E_{oed}, $E_{oed}{}^C$, and $E_{ur}{}^{OED,C}$ and their relations in FS specimens at selected σ'^{ref}_3.

Parameter	Unit	σ'^{ref}_3 [kPa]			
		50	100	200	350
E_0	MN/m²	261.1	391.6	587.4	-
E_{ur}	MN/m²	207.6	316.4	476.3	-
E_{50}	MN/m²	51.02	92.93	169.26	-
E_{oed}	MN/m²	32.8	52.6	93.2	156.2
$E_{oed}{}^C$	MN/m²	21.6	43.3	86.6	151.5
$E_{ur}{}^{OED,C}$	MN/m²	199.9	399.7	799.5	1399
E_{ur}/E_{50}	-	4.1	3.4	2.8	-
E_0/E_{50}	-	5.1	4.2	3.5	-
E_0/E_{ur}	-	1.2	1.3	1.2	-
E_{50}/E_{oed}	-	1.6	1.8	1.8	-
$E_{50}/E_{oed}{}^C$	-	2.4	2.1	2.0	-
$E_{ur}/E_{ur}{}^{OED,C}$	-	1.0	0.8	0.6	-

and Table 2); to enable the comparison, the effective horizontal stress σ'^{ref}_3 was calculated with the equation:

$$\sigma'^{ref}_3 = \sigma'^{ref}_1 \cdot (1 - sin\varphi') \qquad (13)$$

It can be noticed that the relation $E_0 > E_{ur} > E_{50}$ is valid in both materials. The ratio E_{ur}/E_{50} ranges between 3.3 and 4.3 for LSM and 2.8 and 4.1 for FS, which is higher than 2 and lower

than 6 as recommended in the ZSoil manual. The values: 3 for granular soils and 4 for cohesive soils, suggested if no experimental data are available, are within the obtained ranges. On the other hand, the constant value of 3, used in PLAXIS, is underestimated for the loess-sand mixture. The ratio E_0/E_{50} is between 4.9 and 5.7 in LSM and 3.5 to 5.1 in FS, which is within the lower range of 3.6 to 30, but smaller than the typical values of 6 to 14, given by Obrzud & Truty (2020). The E_{50}/E_{oed} ratio is between 2.9 and 3.5 in LSM and between 1.6 and 1.8 in FS, which is inconsistent with the common assumption that these moduli are approximately equal. When E_{oed} is calculated with the approximated Equation (4), using C_C, the discrepancy is even larger. There is no clear relation between the E_{ur} obtained using the basic method and the TX test, and the alternative approach in the OED test. The values of $E_{ur}^{OED,C}$ were equal to E_{ur} at $\sigma'_3 = 350$ kPa in LSM and at 50 kPa in FS; the ratio $E_{ur}/E_{ur}^{OED,C}$ generally increased as confining stress decreased.

The trendlines used to calculate the exponents m_0, m_{50}, m_{ur}, using $\sigma'^{ref}_3 = 100$ kPa, and m_{oed} using $\sigma'^{ref}_1 = 100$ kPa, are showed in Figure 8. Their values, with the corresponding R^2, are listed in Table 5. The trendlines provide reliable approximation of the relations between confining or axial stress and soil stiffness, given that R^2 values are between 0.89 and 1.00. In LSM, the values of the exponent m vary between 0.6 and 0.8, while in FS – between 0.6 and 0.9. They are higher than the commonly assumed value of 0.5 for sands and silts, but agree with the other published results (von Soos, 1991; Kempfert & Gebreselassie, 2006; Surarak et al., 2012). The relations between m and the method of determination, presented by Kempfert & Gebreselassie (2006) and Oztoprak & Bolton (2013), were not confirmed. In LSM, m_{oed} was the highest, followed by m_0 and m_{50}. In FS, the sequence was: $m_{50} > m_{oed} > m_0$. In both materials, m_{ur} was the smallest.

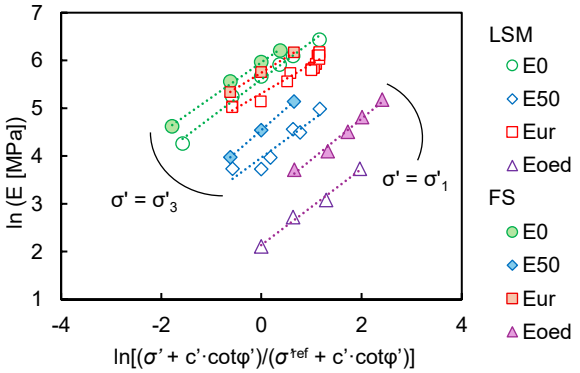

Figure 8. Trendlines used to determine exponents m_0, m_{50}, m_{ur}, m_{oed}.

Table 5. Exponents m and coefficients of determination R^2

		m_0	m_{50}	m_{ur}	m_{oed}
LSM	m	0.789	0.778	0.613	0.799
	R^2	0.989	0.886	0.925	0.989
FS	m	0.736	0.915	0.651	0.850
	R^2	0.996	1.000	0.999	0.984

4 SUMMARY AND CONCLUSIONS

The article presents results of oedometric, triaxial and bender element tests on a loess-sand mixture and a fluvial sand with fines. Selected stiffness parameters, moduli E_0, E_{50}, E_{ur}, and E_{oed}, and the exponent m, necessary to calibrate HS and HSS models, are presented. The relations between the particular parameters are compared with those recommended in the most popular FEM codes.

The results confirm the known relation between the moduli from TX tests: $E_0 > E_{ur} > E_{50}$. Also the ratio E_{ur}/E_{50} is close to the recommended range of 3 to 4. On the other hand, the findings clearly show that the commonly used assumptions that (*i*) E_{50} is equal to E_{oed}, and that (*ii*) the same value of m is obtained regardless of the type of soil and the stiffness modulus used, are not valid for the tested soils. It was also proved that E_{ur} is highly dependent on the methodology of its estimation. The authors recommend that the unloading phase in TX tests be carried out to the stress of at least 1/3 of the stress at the beginning of the loop.

It should be emphasised that due to the complexity of soil behaviour, an optimum calibration of a numerical model requires a very careful choice of both the stress and strain range applied in laboratory tests and the method of interpretation.

REFERENCES

Benz, T. 2007. Small-strain stiffness of soils and its numerical consequences. Ph.D. thesis, University of Stuttgart.

Benz, T., Schwab, R., Vermeer, P. 2009. A small-strain overlay model. *International Journal for Numerical and Analytical Methods in Geomechanics,* 33, 25-44.

Cudny M., and Truty A. 2020. Refinement of the Hardening Soil model within the small strain range. *Acta Geotechnica* 15, 2031–2051.

European Committee for Standardization, 2010. EN 13286-2, Unbound and hydraulically bound mixtures - Part 2: Test methods for laboratory reference density and water content - Proctor compaction.

Gao, Y., Zheng, X., Wang, H., and Luo, W. 2022 Effect of wave attenuation on shear wave velocity determination using bender element tests. *Sensors* 22(3), 1263.

International Organization for Standardization, 2014-2018. ISO 17892, Geotechnical investigation and testing — Laboratory testing of soil.

Janbu, N. 1963. Soil compressibility as determined by oedometer and triaxial tests. In: *Proc. European Conf. SMFE,* Wiesbaden.

Japanese Geotechnical Society, 2000. JGS 0542, Method for cyclic triaxial test to determine deformation properties of geomaterials.

Kempfert, H.G., and Gebreselassie, B. 2006. Excavations and foundations in soft soils. Berlin, Heidelberg: Springer Berlin Heidelberg.

Kowalska, M., and Vrettos Ch. 2025. Bender element tests on sand-rubber mixtures – effects of interpretation procedure and loading sequence. Geosynthetics International (*in review*)

Obrzud, R., and Truty, A. 2020. *ZSoil for geotechnics & structures. The hardening soil model. A practical guidebook*. Report 100701. Switzerland: GeoDev.

Oztoprak, S., and Bolton, M.D. 2013. Stiffness of sands through a laboratory test database. *Géotechnique* 63(1), 54-70.

PLAXIS. 2024. *Plaxis 2D 2024.3. Material Models Manual 2D.* Bentley.

Rebolledo, J.F.R., León, R.F.P., and Camapum de Carvalho, J. 2019. Obtaining the mechanical parameters for the hardening soil model of tropical soils in the city of Brasília. *Soils and Rocks* 42(1), 61-74.

Schanz, T., Vermeer, P.A., and Bonnier, P.G. 1999. The hardening soil model: Formulation and verification. In: *Beyond 2000 in computational geotechnics – 10 Years of PLAXIS*. Rotterdam: Balkema.

Surarak, C., Likitlersuang, S., Wanatowski, D., Balasubramaniam, A., Oh, E., and Guan, H. 2012. Stiffness and strength parameters for hardening soil model of soft and stiff Bangkok clays. *Soils and Foundations* 52(4), 682-697.

Tankiewicz, M., Kowalska, M., Mońka, J. 2024. Evaluation of shear strength and stiffness of a loess–sand mixture in triaxial and unconfined compression tests. *Materials* 17(15), 3831.

Vermeer, P.A., and Meier, C.P. 1998. Stability and deformations in deep excavations in cohesive soils. In: *Proceedings of International Conference on Soil-Structure Interaction in Urban Civil Engineering*, Darmstadt Geotechnics.

Viggiani, G., and Atkinson, J. H. 1995. Stiffness of fine-grained soil at very small strains. *Géotechnique* 45(2), 249-265.

Von Soos, P. 1991. Grundbataschenbuch, Berlin: Ernst & Sohn.